

University of Groningen

Effect of Different EndoAnchor Configurations on Aortic Endograft Displacement Resistance

Goudekettering, Seline R.; Vermeulen, Jenske J. M.; van Noort, Kim; Scholten, Gerben te Riet
 o g; Kuipers, Henny; Slump, Cornelis H.; de Vries, Jean-Paul P. M.

Published in:
 Journal of Endovascular Therapy

DOI:
[10.1177/1526602819857586](https://doi.org/10.1177/1526602819857586)

IMPORTANT NOTE: You are advised to consult the publisher's version (publisher's PDF) if you wish to cite from it. Please check the document version below.

Document Version
 Publisher's PDF, also known as Version of record

Publication date:
 2019

[Link to publication in University of Groningen/UMCG research database](#)

Citation for published version (APA):

Goudekettering, S. R., Vermeulen, J. J. M., van Noort, K., Scholten, G. T. R. O. G., Kuipers, H., Slump, C. H., & de Vries, J-P. P. M. (2019). Effect of Different EndoAnchor Configurations on Aortic Endograft Displacement Resistance: An Experimental Study. *Journal of Endovascular Therapy*.
<https://doi.org/10.1177/1526602819857586>

Copyright

Other than for strictly personal use, it is not permitted to download or to forward/distribute the text or part of it without the consent of the author(s) and/or copyright holder(s), unless the work is under an open content license (like Creative Commons).


The publication may also be distributed here under the terms of Article 25fa of the Dutch Copyright Act, indicated by the "Taverne" license. More information can be found on the University of Groningen website: <https://www.rug.nl/library/open-access/self-archiving-pure/taverne-amendment>.

Take-down policy

If you believe that this document breaches copyright please contact us providing details, and we will remove access to the work immediately and investigate your claim.

Downloaded from the University of Groningen/UMCG research database (Pure): <http://www.rug.nl/research/portal>. For technical reasons the number of authors shown on this cover page is limited to 10 maximum.

Effect of Different EndoAnchor Configurations on Aortic Endograft Displacement Resistance: An Experimental Study

Journal of Endovascular Therapy
 1–10
 © The Author(s) 2019
 Article reuse guidelines:
sagepub.com/journals-permissions
 DOI: 10.1177/1526602819857586
www.jevt.org


Seline R. Goudekettig, MSc^{1,2*} , Jenske J. M. Vermeulen, MSc^{1,2*},
 Kim van Noort, MSc^{1,2}, Gerben te Riet o. g. Scholten, Ing³, Henny Kuipers³,
 Cornelis H. Slump, MSc, PhD², and Jean-Paul P. M. de Vries, MD, PhD⁴

Abstract

Purpose: This study investigated the effect of different EndoAnchor configurations on aortic endograft displacement resistance in an in vitro model. **Materials and Methods:** An in vitro model was developed and validated to perform displacement force measurements on different EndoAnchor configurations within an endograft and silicone tube. Five EndoAnchor configurations were created: (1) 6 circumferentially deployed EndoAnchors, (2) 5 EndoAnchors within 120° of the circumference and 1 additional, contralateral EndoAnchor, (3) 4 circumferentially deployed EndoAnchors, (4) 2 rows of 4 circumferentially deployed EndoAnchors, and (5) a configuration of 2 columns of 3 EndoAnchors. An experienced vascular surgeon deployed EndoAnchors under C-arm guidance at the proximal sealing zone of the endograft. A constant force with increments of 1 newton (N) was applied to the distal end of the endograft. The force necessary to displace a part of the endograft by 3 mm was defined as the endograft displacement force (EDF). Two video cameras recorded the measurements. Videos were examined to determine the exact moment 3-mm migration had occurred at part of the endograft. Five measurements were performed after each deployed EndoAnchor for each configuration. Measurements are given as the median and interquartile range (IQR) Q1, Q3. **Results:** Baseline displacement force measurement of the endograft without EndoAnchors resulted in a median EDF of 5.1 N (IQR 4.8, 5.2). The circumferential distribution of 6 EndoAnchors resulted in a median EDF of 53.7 N (IQR 49.0, 59.0), whereas configurations 2 through 5 demonstrated substantially lower EDFs of 29.0 N (IQR 28.5, 30.1), 24.6 N (IQR 21.9, 27.2), 36.7 N, and 9.6 N (IQR 9.4, 10.0), respectively. Decreasing the distance between the EndoAnchors over the circumference of the endograft increased the displacement resistance. **Conclusion:** This in vitro study demonstrates the influence EndoAnchor configurations have on the displacement resistance of an aortic endograft. Parts of the endograft where no EndoAnchor has been deployed remain sensitive to migration. In the current model, the only configuration that rivaled a hand-sewn anastomosis was the one with 6 EndoAnchors. A circumferential distribution of EndoAnchors with small distances between EndoAnchors should be pursued, if possible. This study provides a quantification of different EndoAnchor configurations that clinicians may have to adopt in clinical practice, which can help them make a measured decision on where to deploy EndoAnchors to ensure good endograft fixation.

Keywords

displacement force, endoanchor, endograft, endoleak, fixation, in vitro model, migration, proximal neck, sealing zone, stent-graft

Introduction

Circumferential seal is a key factor in the prevention of proximal neck-related complications after endovascular aneurysm repair (EVAR).¹ Despite the improvement in endografts (eg, suprarenal fixation and anchoring hooks and pins), migration remains a complication that may lead to late type Ia endoleak.^{2–5} Spanos et al⁵ demonstrated a 8.6%

migration rate after EVAR, of which 22.4% of cases had concomitant type I endoleak.

Experimental studies have assessed the displacement forces to better understand proximal fixation of various types of endografts.^{6–10} Although endografts with anchoring hooks and pins demonstrated higher displacement forces than endografts without these fixation modalities,

the displacement force was less than the 56 newtons (N) that could be achieved with a conventional hand-sewn anastomosis.^{7,9}

The Heli-FX EndoAnchor System (Medtronic Vascular, Santa Rosa, CA, USA) was developed to improve sealing and increase the migration resistance of an endograft after EVAR.^{11–14} The helically shaped EndoAnchors should be deployed through the endograft into the aortic wall. The instructions for use (IFU) recommend at least 4 or 6 EndoAnchors for neck diameters of ≤ 29 mm or > 29 mm, respectively; a circumferential deployment is advised.^{7,11}

Melas et al⁷ analyzed the effect on displacement force of the endograft after circumferentially deploying 4 or 6 EndoAnchors. The addition of EndoAnchors significantly increased the force to dislodge all endografts, approximating the strength of a surgical hand-sewn anastomosis. Circumferential distribution of EndoAnchors may, however, not always be possible due to highly calcified regions, thrombus, or severe aortic neck angulation.^{15,16} Moreover, therapeutic use of EndoAnchors is mostly targeted to the location of the complication; EndoAnchors will be deployed in and close to the location of the type Ia endoleak. The remaining EndoAnchors in the cassette are not always used; hence, circumferential distribution may not be achieved. The effect of these different distributions on displacement forces remains unknown.¹⁷ Understanding the consequence of these different distributions is important because they may result in late complications.^{18,19} Therefore, the aim of this in vitro study was to investigate the effect of different EndoAnchor configurations on proximal endograft displacement when a constantly increasing force is applied.

Materials and Methods

Experimental Setup

An experimental setup was developed to perform longitudinal force measurements; a schematic overview is shown in Figure 1. A silicone tube (VMQ 60° Shore A; Peter van den Berg Afdichtingstechnieken B.V., Barendrecht, the Netherlands) with a wall thickness of 1 mm and an inner diameter of 24 mm was used in this in vitro model to simulate the aortic neck. The same silicone tube material was used for all the measurements that allowed for adequate assessment of the displacement forces. A new silicone tube

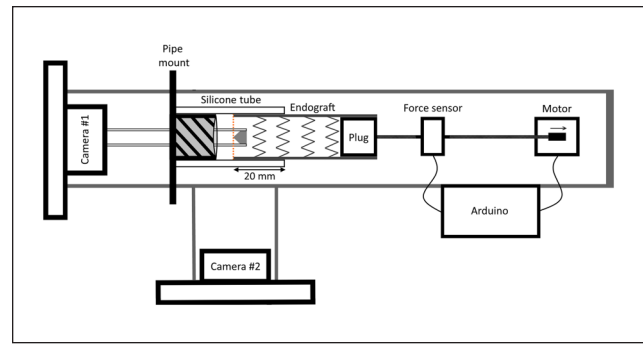


Figure 1. Schematic view (from above) of the experimental setup. The silicone tube was affixed to the pipe mount, and the endograft was deployed within the silicone tube. A 20-mm sealing zone was achieved. The orange dotted line designates the top of the fabric. The pulling mechanism, consisting of the plug and cord, was attached to a force sensor, which in turn was connected to the motor by a similar cord. An Arduino board controlled the motor and was programmed to stop the motor when 3-mm migration of a part of the endograft was achieved. The endograft displacement was visualized and recorded by 2 cameras.

was used for each of the configurations. The silicone tube was fastened on a rigid pipe mount in the setup.

A 30-mm Valiant Thoracic Stent Graft (Medtronic Vascular) with the bare stent removed was deployed in the silicone tube. Removal of the bare stent and anchoring pins prevented damage to the silicone tube and created comparable measurements based on the outward radial force of the stent alone, such that only the effect of the additional value of the EndoAnchors could be observed. A tube stent-graft was used to create an equal distribution of the displacement force of the pulling mechanism in this in vitro model.

The pulling mechanism consisted of a plug attached to a cord that was able to withstand a force of 100 N. The plug was fixed into the distal end of the endograft and the cord connected to a force sensor (Z-SG; Seneca, Padua, Italy) that continuously measured the applied force. On the other end of the force sensor, a similar cord was connected to the motor (Herkulex DRS 0402; Dongbu Robot, Chungcheongnam-do, South Korea). The motor induced a constant longitudinal force on the pulling mechanism. An Arduino Mega 2560 board (Arduino, Cham, Switzerland) was programmed to control the motor and receive the measured forces of the

¹Department of Vascular Surgery, St Antonius Hospital, Nieuwegein, the Netherlands

²MIRA Institute of Biomedical Technology and Technical Medicine, University of Twente, Enschede, the Netherlands

³Robotics and Mechatronics, Faculty of Electrical Engineering, Mathematics & Computer Science, University of Twente, Enschede, the Netherlands

⁴Department of Surgery, Division of Vascular Surgery, University Medical Centre Groningen, the Netherlands

*Seline R. Goudekettering and Jenske J. M. Vermeulen contributed equally to this work and have shared first authorship.

Corresponding Author:

Seline R. Goudekettering, Department of Vascular Surgery, St Antonius Hospital, Koekoekslaan 1, 3435 CM, Nieuwegein, the Netherlands.
Email: goudekettering38@gmail.com

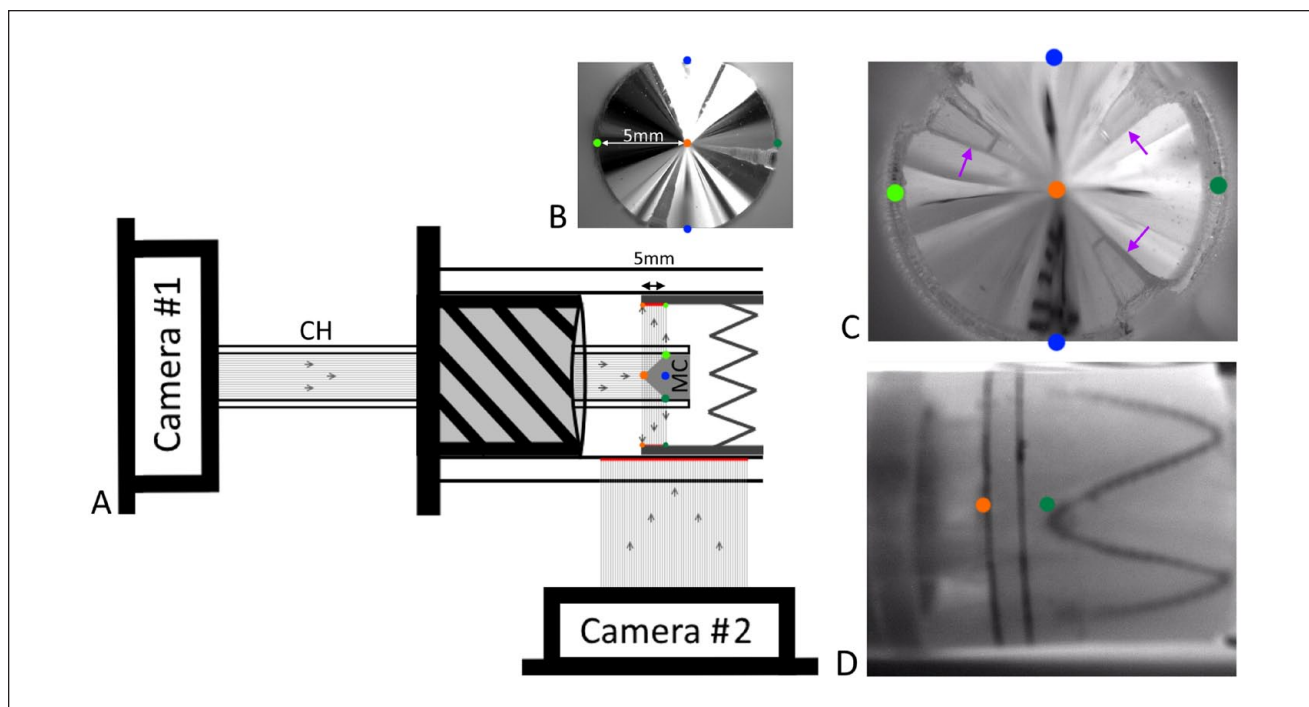


Figure 2. Schematic representation of the visualization of the proximal part of the endograft. (A) Camera 1 was aimed at a mirror cone (MC) that is fixed by the cone holder (CH). The camera image was reflected by the mirror cone onto the proximal part of the endograft, creating a 360° view of the proximal 5 mm of the endograft. The apex of the cone (orange dot) is located in the center of the frame, whereas the base of the cone is located on the outer edge of the frame (green and blue dots). (B) The point of view of camera 1 is solely the mirror cone. The orientation in the image is the same as that of the camera, represented by the corresponding color dots in the schematic overview. (C) Point of view of camera 1. An image frame of the proximal part of the endograft that was deployed as presented in A. Note that the point of view is the same as in B. The mirror cone is held in place by 3 transparent fixation bars (purple arrows). (D) Point of view from camera 2 (the left side of the endograft). The 2 lines represent 3-mm displacement, the distance between the orange and green dots is 5 mm (similar to that visualized by camera 1).

force sensor. A safety mechanism was built into the Arduino to automatically stop and release traction of the motor when a sudden rapid decrease in force was recorded by the force sensor or if the force reached 60 N (ie, greater than a hand-sewn anastomosis^{7,9} and therefore considered sufficient).

Two video cameras (mvBlueFox-IGC202bG; Matrix Vision, Oppenweiler, Germany) recorded the proximal part of the endograft; camera 1 visualized the inside and camera 2 the outside. Dedicated software developed in-house in MATLAB 2015b (MathWorks, Natick, MA, USA) controlled the Arduino and both cameras. The visualization of the cameras is displayed in more detail in Figure 2. Camera 1 included a 1280×960-pixel resolution and 10×10-mm field of view (FOV) recorded at 12.3 frames per second (fps). This camera was aimed at a mirror cone (Figure 2A), which was fixed by the cone holder (Figure 2A). The mirror cone had a diameter of 10 mm and height of 5 mm, resulting in a 5-mm-wide reflection onto the inside of the endograft. By use of the mirror cone, the camera gives a 360° view of the inside of the endograft with a radius of 5 mm. When a single image is taken with

camera 1, the apex of the cone can be seen in the middle of the frame (Figure 2A and B), whereas the base of the cone is visualized on the outer edge of the image. The point of view of the camera corresponds to that of the image that is taken (Figure 2B). Thus, left and right correspond to left and right in the image frame, and the same applies to the top and bottom of the image. Camera 2 (1280×960-pixel resolution, 33×33-mm FOV, 12.3 fps) was set up at a fixed distance of 15.3 cm perpendicular to the silicone tube and endograft. The obtained image from the point of view of cameras 1 and 2 can be seen in Figure 2C and D.

Figure 3 shows an example of a measurement with endograft displacement visualized by both cameras. A schematic representation of the endograft starting point (Figure 3A) and after 3-mm migration (Figure 3D) can be seen. The proximal part of the endograft was deployed within the silicone tube with a 20-mm sealing length (Figure 3C). The most proximal part of the endograft corresponded to the apex of the cone (Figure 3A); thus, the endograft displacement started from the center of the frame created by camera 1 (Figure 3B). During the measurements, the motor applied

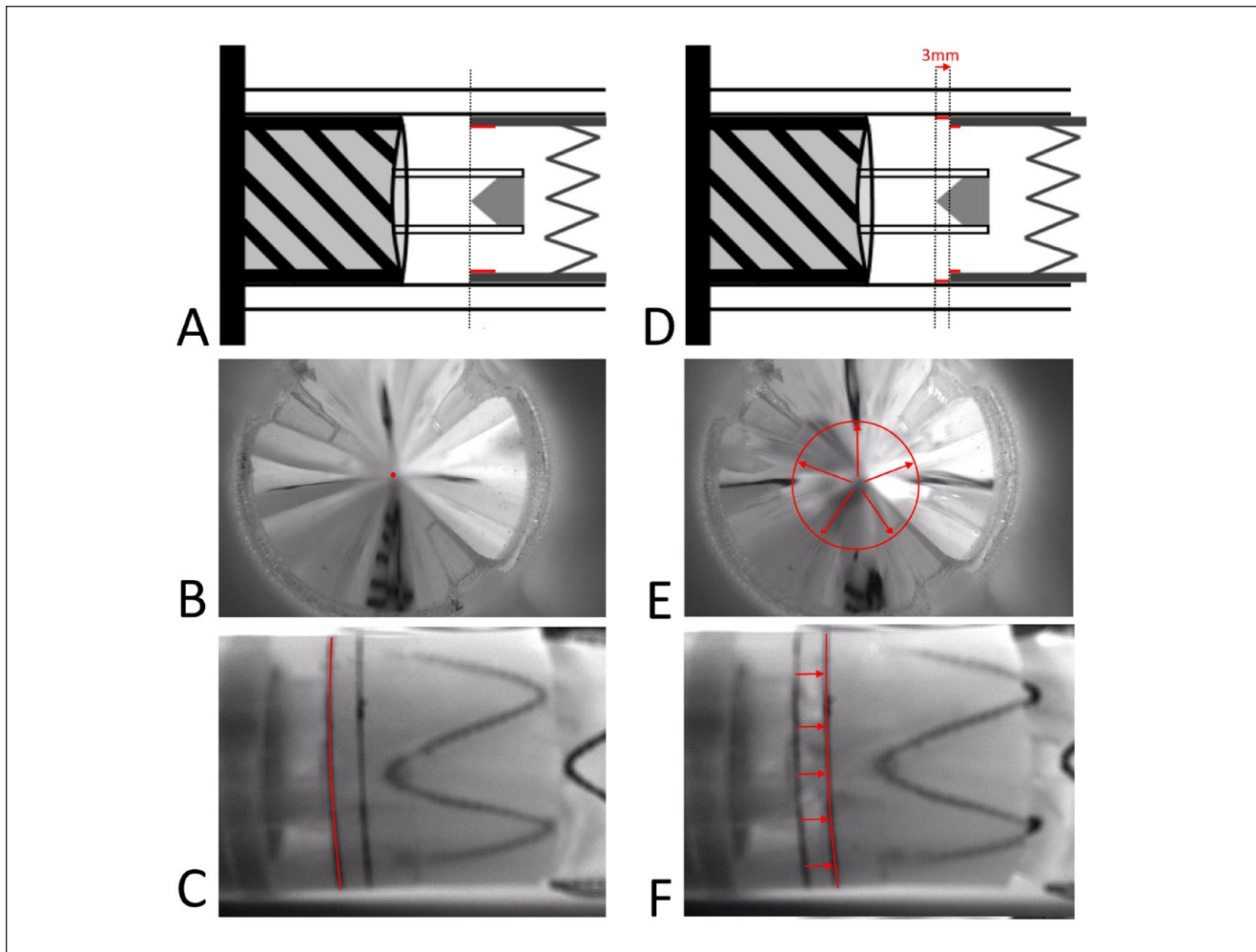


Figure 3. Example of endograft displacement visualized from both cameras (camera 1 in panels B and E, camera 2 in panels C and F). (A) Schematic representation of the endograft in the starting position with 20 mm of proximal apposition (dotted black line indicates the top of the fabric). The most proximal part of the endograft corresponds to the apex of the cone. (B) Point of view from camera 1 on the mirror cone. Endograft migration will start from the center of the image frame. (C) Point of view from camera 2 showing the starting position with 20 mm of apposition. (D) Schematic representation of the endograft after 3-mm migration has occurred. (E) Gradual endograft migration toward the outer edge of the image (ie, the base of the cone). (F) Gradual endograft migration toward the force (ie, right). The video of this measurement is available online as Supplementary Video 1.

traction to gradually increase the force in increments of 1 N. This resulted in a gradual displacement of the endograft toward the outer edge of the image (Figure 3E) and toward the left of the image (Figure 3F). The endograft displacement force (EDF) was defined as the force necessary to displace part of the endograft by 3 mm. A displacement of 3 mm was chosen because it is assumed to be clinically relevant and is enough to demonstrate the location of migration but also allows for repeatable measurements.

The measurements were manually stopped when visual inspection showed 3-mm migration of a part of the endograft. However, the measurements were also automatically stopped when one of the Arduino's safety mechanisms was activated (see below). If the applied force resulted in

macroscopic damage to the silicone tube or endograft (because of the insertion of EndoAnchors) or to the EndoAnchors, the following measurements were performed with a new silicone tube, endograft ring, and EndoAnchors. The visualization from cameras 1 and 2 of the measurement depicted in Figure 3 can be found in Supplementary Video 1 (available in the online version of the article).

Validation of the Experimental Setup

Before the measurements were performed, the force sensor was validated with weights of a known mass, and a linear relationship was observed (Figure 4). The built-in safety mechanisms of the Arduino were tested to automatically stop when

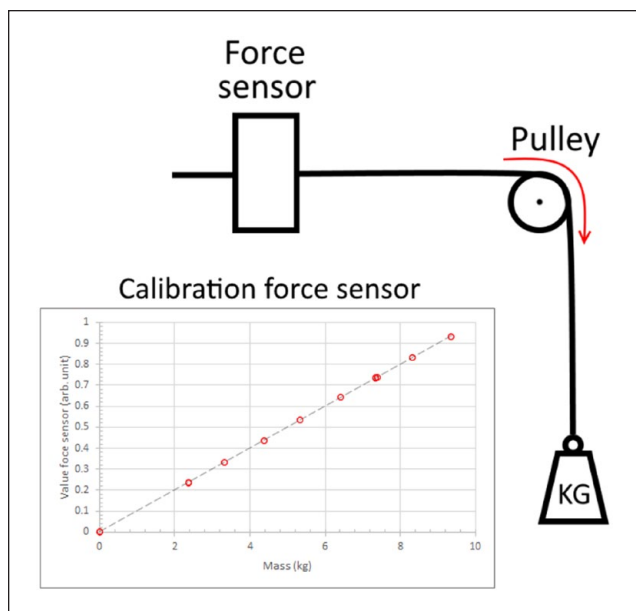


Figure 4. Schematic representation of the calibration of the force sensor. Weights with a known mass were varied between 0 and 10 kg, demonstrating a linear correlation between the force sensor and the known weights.

the force exceeded 60 N or if the force sensor experienced a rapid decrease in force (≥ 2 N per measurement point of the force sensor). The software program was tested to control the cameras to make sure that both cameras recorded simultaneously. Moreover, a 1-mm calibration grid was placed into the silicone tube to record the amount of elongation observed by camera 1. Tearing and deformation of the silicone tube was evaluated when a force up to 80 N was applied. The silicone was able to withstand this force without tearing. Moreover, holes similar to that of a penetrating EndoAnchor did not result in deformation or tearing of the silicone.

To analyze the repeatability of the experimental setup, 1 observer performed 2 sets of 25 measurements (spread out over 2 days), where 1 EndoAnchor was deployed within an Endurant endograft without oversizing. A mean difference of 0.1 N was observed between the measurements, with 95% of the dispersion within 0.4 N.

Displacement Force Measurements

First, a set of 5 baseline measurements was performed without EndoAnchors to assess the EDF. The median of these measurements served as the baseline value.

Based on thorough clinical evaluation of a previous patient cohort in patients treated by EndoAnchors in a therapeutic setting,²⁰ 5 configurations were created with different distributions along the circumference to investigate the effect of EndoAnchor distribution on proximal endograft displacement resistance (Figure 5: 1F, 2F, 3D, 4C/D, and

5A/B). To establish the EDF, a set of 5 measurements was performed after deployment of each EndoAnchor. After these 5 measurements were performed, a new EndoAnchor was added to the model, and another set of 5 measurements was performed. A total of 18 different EndoAnchor distributions patterns were assessed (Figure 5). All EndoAnchors were deployed by an experienced vascular surgeon.

Endoanchor Configurations

Configuration 1 is the circumferential deployment of 6 EndoAnchors (Figure 5: 1A-F), according to recommended use in large (>29 mm) aortic neck diameters. It represents the ideal EndoAnchor deployment for prophylactic cases. Configuration 2 is frequently observed in therapeutic use to treat type Ia endoleaks. The EndoAnchors are deployed at the location of the endoleak, often within 120° of the circumference (Figure 5: 2A-E). The effect of deploying one additional EndoAnchor on the contralateral side was also investigated (Figure 5; 2F).

For prophylactic use of EndoAnchors in aortic neck diameters ≤ 29 mm, 4 circumferential EndoAnchors are recommended. However, this exact circumferential distribution may be hard to achieve during deployment. Thus, the effect of an almost circumferential distribution (ie, the closest distance was 60° and the largest was 120°) was investigated in the third configuration (Figure 5: 3A-D).

The fourth configuration has 2 rows of 4 circumferential EndoAnchors to represent the ideal placement (ie, 90° between the EndoAnchors) for prophylactic use, with an additional row of EndoAnchors (Figure 5: 4A/B). It may be argued that a second row of EndoAnchors can reinforce displacement resistance but especially will increase the length of the seal zone in the infrarenal neck.

Configuration 5 (Figure 5: 5A-D) was designed to demonstrate the effect of deploying EndoAnchors in a row, as in case of the treatment of a type Ia endoleak associated with gutters in a chimney-EVAR procedure.

Statistical Analysis

Normality of the data was assessed with the Shapiro-Wilk test. Continuous data are reported as median and interquartile range (IQR Q1, Q3). The videos were examined to determine the effect of the forces induced on the endograft, EndoAnchor, and silicone tube. Statistical analyses were performed with SPSS software (version 24; IBM Corporation, Armonk, NY, USA).

Results

Displacement Force Measurements

The baseline measurements resulted in a median EDF of 5.1 N (IQR 4.8, 5.2). The measured EDFs to displace a

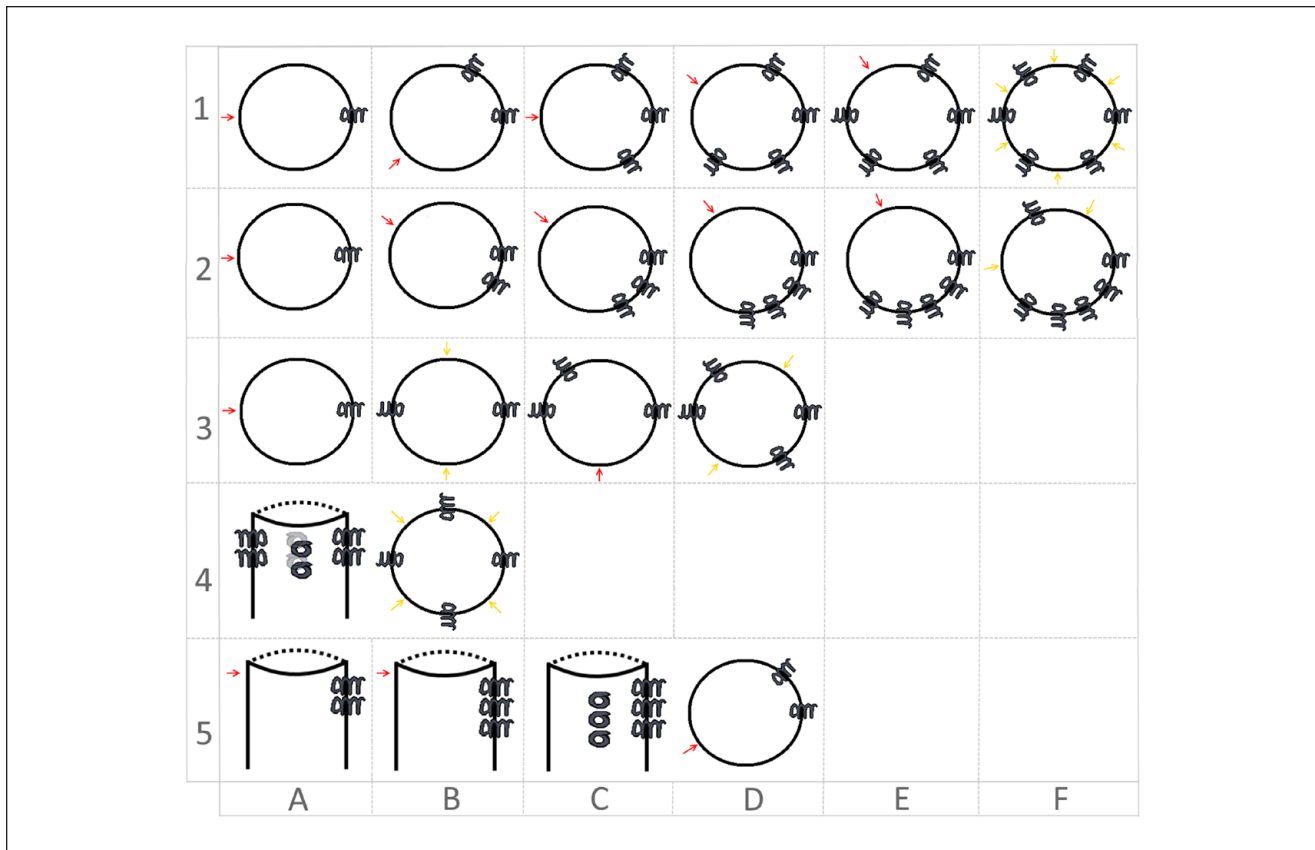


Figure 5. Schematic representation of the different EndoAnchor configurations. The red arrows point to the location where the 3-mm displacement is expected to occur first. The yellow arrows point to equal circumferential distances between the EndoAnchors; 3-mm displacement is expected to occur at any of these locations. (1A-F) Building up to a circumferential distribution. (2A-F) Configuration mainly used therapeutically in the case of type Ia endoleaks. (3A-D) A distribution of 4 EndoAnchors, where the effect of a noncircumferential distribution is investigated. (4A/B) Circumferential distribution with the addition of an extra row of circumferentially deployed EndoAnchors. Of note, 4B is the view from above the configuration achieved in 4A. (5A-D) Configuration used in the treatment or prevention of gutters after a chimney endovascular aneurysm repair procedure. Of note, 5D is the view from above of the configuration achieved in 5C.

part of the endograft by 3 mm for the different EndoAnchor configurations are provided in Table 1. The deployment of a single EndoAnchor increased the median EDF from 5.1 to 7.9 N. The first 2 EndoAnchors of configuration 1 are rather similar, whereas adding EndoAnchors 3 to 6 substantially increased the EDF. Notice the large increase in median EDF between 5 and 6 EndoAnchors (ie, 26.7 and 53.7 N, respectively). The addition of the sixth EndoAnchor, thereby decreasing the maximum circumferential distance between EndoAnchors from 120° to 60°, increased the EDF by 27 N.

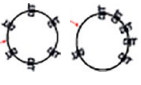




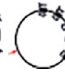









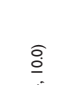
The use of 1 to 3 EndoAnchors within 90° of the circumference (Table 1; configuration 2) demonstrated a minor increase in median EDF of 8.2 to 9.8 N. Extending the coverage up to 120° (by adding 2 more EndoAnchors) increased the median EDF to 17.5 N. The deployment of the sixth EndoAnchor in configuration 2 substantially increased the EDF to a median of 29.0 N.

The addition of each EndoAnchor within configuration 3 had a considerable effect on the EDF, possibly because of the decrease in the uncovered area between the EndoAnchors. The addition of the fourth EndoAnchor reduced the area to approximately 120°; hence, the EDF becomes similar to the EDF of configuration 1 with 5 EndoAnchors.

Owing to macroscopic damage to the silicone tube and endograft, configuration 4 could be measured only once due to limited availability of materials. The median EDF from the 5 measurements was 36.7 N, which is higher than the median EDF of 24.6 N of 4 EndoAnchors in configuration 5. This may be associated with the more equal distribution of space between EndoAnchors (ie, 90° in configuration 4 vs 120° in configuration 5).

In configuration 5, creating a column of 2 or 3 EndoAnchors resulted in nearly the same EDF as that of 1 EndoAnchor. The addition of the second column (just like in the treatment of gutters near a chimney) increased the

Table 1. The Endograft Displacement Force to Displace (a Part of) the Endograft by 3 mm.^a

Configuration	Endograft Displacement Force, N									
1	7.5 (7.1, 7.7)	8.1 (7.8, 8.1)	10.6 (9.8, 11.0)	23.6 (22.4, 24.4)	26.7 (26.5, 27.6)	53.7 (49.0, 59.0)				
2	8.2 (7.4, 8.3)	9.2 (8.7, 9.4)	9.8 (9.7, 10.3)	12.2 (11.7, 12.4)	17.5 (17.1, 17.8)	29.0 (28.5, 30.1)				
3	8.0 (7.8, 8.4)	11.5 (11.2, 11.7)	18.0 (17.5, 18.8)	24.6 (21.9, 27.2)						
4	7.9 (7.5, 8.2)									
5	8.1 (7.9, 8.3)	7.7 (7.6, 7.8)	9.6 (9.4, 10.0)							

^aData are presented as median (interquartile range Q1, Q3). The red arrows point to the location where the endograft displacement force was measured.

^bMeasured only once due to macroscopic damage to the silicone tube and endograft.

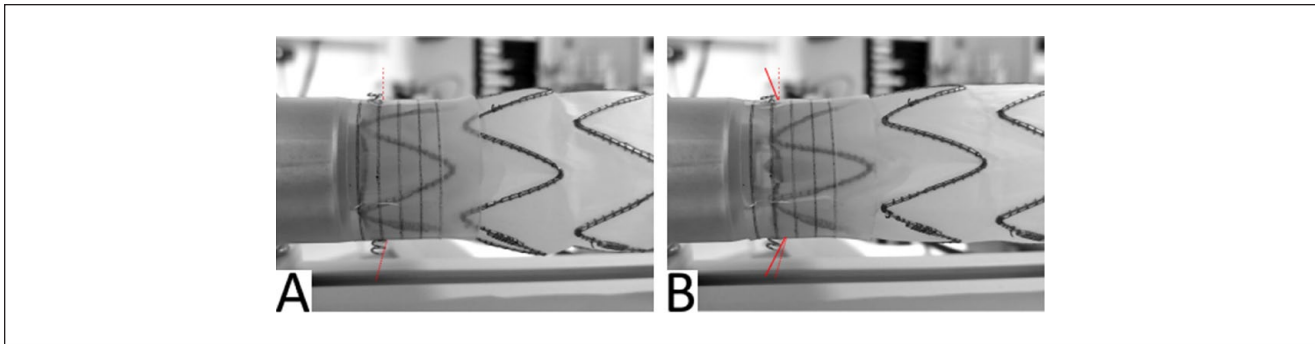


Figure 6. Positional changes of the EndoAnchors during the measurements. (A) The measurement starting point, with the angle of the EndoAnchor (dotted red line). (B) The endograft after 3-mm migration. Notice the change in position of both EndoAnchors when the endograft displacement force is achieved (solid red lines).

EDF. Nevertheless, the median EDF was 9.6 N, comparable to that of 3 EndoAnchors of configuration 2 (median 9.8 N), possibly because the distance in between the EndoAnchors of both of these configurations was similar, and a large part of the circumference was not fixated with EndoAnchors.

Video Analyses

As expected, the largest endograft displacement areas were those on the side opposite of where the EndoAnchors were deployed (see Supplementary Video 2; available in the online version of the article). When 6 EndoAnchors were circumferentially deployed (configuration 1), the EDF was larger than when 6 EndoAnchors were noncircumferentially distributed (eg, configuration 2). Decreasing the distance between the EndoAnchors resulted in a higher displacement resistance. Lastly, as visualized by camera 2 (Figure 6), the EndoAnchors tilted during the measurements when the displacement force was applied.

Discussion

This in vitro study analyzed the effect of different EndoAnchor configurations on proximal endograft displacement resistance. Circumferential deployment of 6 EndoAnchors demonstrated an EDF greater than a hand-sewn anastomosis. A gap $>90^\circ$ between 2 EndoAnchors along the circumference led to a substantially lower displacement force. Decreasing the distance between EndoAnchors is important to increase the displacement resistance.

Thorough analysis of follow-up data from patients treated with EndoAnchors for type Ia endoleaks in a therapeutic setting showed multiple distribution patterns, many of which were noncircumferential because of the targeted use of the EndoAnchors at the location of the type Ia endoleak.²⁰ For this study, the recommended circumferential distribution was chosen as well as these frequently

observed therapeutic configurations. The endograft remained prone to migration at the locations along the circumference that were not anchored by EndoAnchors, as was hypothesized.

The IFU recommend deployment of at least 4 or 6 EndoAnchors.^{14,18,21} Although more EndoAnchors are deployed in a therapeutic setting compared with a prophylactic setting,²⁰ a number of EndoAnchors in the 10-anchor cassette often remain unused in both scenarios. Based on the configurations observed in previous research in therapeutically treated patients,²⁰ 5 configurations were chosen for this in vitro study. When EndoAnchors have resolved a complication in therapeutic cases, the remaining EndoAnchors should be deployed to reduce the circumferential distance between EndoAnchors and to increase the EDF. Merely using EndoAnchors in a targeted manner does not result in an EDF comparable to circumferential deployment. Although no complication is being treated in a prophylactic setting, use of more EndoAnchors to reduce the circumferential distance between EndoAnchors can increase the EDF. Therefore, this would suggest using at least 6 EndoAnchors evenly divided along the circumference, which applies to both prophylactic and therapeutic cases. Although not investigated in this study, using all 10 EndoAnchors available in the cassette may further increase the EDF.

EVAR is associated with an early survival benefit when compared with open repair. In the long term, however, this benefit is lost, and durability is inferior to that of open repairs.²² The use of EndoAnchors can prevent and treat type Ia endoleaks and migration, demonstrating significant sac regression at 2-year follow-up.^{14,18,19,23} Consistent prophylactic use of EndoAnchors to create an endovascular suture line may reduce late EVAR failures, thereby possibly also reducing the need for reinterventions.

Earlier research demonstrated that nearly 30% of implanted EndoAnchors did not penetrate the aortic wall in therapeutically treated patients.¹⁷ This study demonstrated

that when there are larger areas along the circumference without EndoAnchor deployment (similar to a nonpenetrating EndoAnchor), the EDF will be substantially lower. In addition, the effect of borderline or nonpenetrating EndoAnchors will be less hazardous if the total number of implanted EndoAnchors is greater. To create a high EDF, good preoperative planning is of utmost importance to make sure that all EndoAnchors are deployed circumferentially and penetrate the aortic wall.

In addition, an endograft oversized too much (>25%) can result in folds that can hamper deployment and penetration of the EndoAnchors in the aortic wall. In the current study, the EndoAnchor penetration depth was less when deployed through 2 layers of fabric (folds). This may be an explanation for the <2-mm EndoAnchor penetration depths (or borderline penetrating EndoAnchors) reported in a recent clinical study.²⁰ The effect of this shorter penetration depth was not investigated in this study.

A distribution that may increase the EDF is one in which EndoAnchors are deployed in a staggered, 2-row configuration. Such a distribution may also increase the seal length in the neck, which may be crucial in short, conical aortic necks. Furthermore, many patients receiving EndoAnchors have one or more challenging aortic neck characteristics.^{14,18,19,21} Especially in these patients, with an already increased risk for migration and type Ia endoleaks, using all available EndoAnchors and a second row of EndoAnchors may prove beneficial because the apposition in the neck can be increased. However, more configurations should be tested to investigate this supposition.

It should be noted that the actual EndoAnchor deployment was slightly different from the ideal EndoAnchor configurations. Even in the hands of an experienced vascular surgeon, the location of the deployed EndoAnchors deviated slightly from the ideal configurations. In addition, stent wires could hinder the intended location of EndoAnchor deployment. However, this mimics a clinical setting.

Limitations

In this in vitro model, the bare stent with anchoring pins was removed to be able to reuse the endograft and create comparable circumstances during the repeated measurements. Because of this modification of the endograft, the EDF will be lower than in a real clinical setting. Moreover, 1 row of the endograft struts was used for every measurement. When a configuration was completed, the row was removed and the subsequent row was used for the following configuration. This could have altered the endograft integrity and could have negatively influenced the EDF. Because of macroscopic damage to the silicone tube and endograft and the limited set of materials, configuration 4 could be measured only once. Ideally, a new endograft would have been used for every configuration. In addition,

only a straight silicone tube was used during the measurements, and the effect of other types or shapes (eg, angulated, conical, or tapered) of silicone tubes was not investigated.

The 3-mm migration was determined by visual inspection and analysis of the video recordings, which might have introduced bias. An upgrade of the experimental setup by automatic detection and tracking of the top of the endograft and an automatic stop of the motor after 3-mm migration has occurred could overcome this bias.

The goal of this study was to investigate the effect on displacement from adding EndoAnchors to distributions rather than to analyze the force necessary to displace an endograft. This setup sufficed for this purpose, but these results cannot be compared to that of other experimental studies investigating the dislodgement force of an endograft.^{6–10,24,25}

Conclusion

This in vitro study demonstrates the influence of different EndoAnchor configurations on the displacement resistance of an aortic endograft. Parts of the endograft where no EndoAnchor has been deployed remain sensitive to migration. In the current model, the only configuration that rivaled a hand-sewn anastomosis was the one with 6 EndoAnchors. A circumferential distribution of EndoAnchors with small distances between the EndoAnchors should be pursued if possible. This study provides a quantification of different EndoAnchor configurations that a clinician may have to adopt in clinical practice, which can help them make a measured decision on where to deploy EndoAnchors to ensure good endograft fixation.

Declaration of Conflicting Interests

The author(s) declared no potential conflicts of interest with respect to the research, authorship, and/or publication of this article.

Funding

The author(s) received no financial support for the research, authorship, and/or publication of this article.

Supplemental Material

The videos are available at <http://journals.sagepub.com/doi/suppl/10.1177/1526602819857586>

ORCID iD

Seline R. Goudekettig  <https://orcid.org/0000-0003-2565-7482>

References

1. de Almeida MJ, Yoshida WB, Hafner L, et al. Factors involved in the migration of endoprosthesis in patients undergoing endovascular aneurysm repair. *J Vasc Bras*. 2010;9:61–71.

2. Daye D, Walker TG. Complications of endovascular aneurysm repair of the thoracic and abdominal aorta: evaluation and management. *Cardiovasc Diagn Ther*. 2018;8(suppl 1):S138–S156.
3. Greenberg RK, Turc A, Haulon S, et al. Stent-graft migration: a reappraisal of analysis methods and proposed revised definition. *J Endovasc Ther*. 2004;11:353–363.
4. Filis KA, Galyfos G, Sigala F, et al. Proximal aortic neck progression: before and after abdominal aortic aneurysm treatment. *Front Surg*. 2017;4:23. doi:10.3389/fsurg.2017.00023
5. Spanos K, Karathanos C, Athanasoulas A, et al. Systematic review of follow-up compliance after endovascular abdominal aortic aneurysm repair. *J Cardiovasc Surg (Torino)*. 2018;59:611–618.
6. Bosman WMPF, van der Steenhoven TJ, Suárez DR, et al. The proximal fixation strength of modern EVAR grafts in a short aneurysm neck. An in vitro study. *Eur J Vasc Endovasc Surg*. 2010;39:187–192.
7. Melas N, Perdikides T, Saratzis A, et al. Helical EndoStaples enhance endograft fixation in an experimental model using human cadaveric aortas. *J Vasc Surg*. 2012;55:1726–1733.
8. Andrews SM, Anson AW, Greenhalgh RM, et al. In vitro evaluation of endovascular stents to assess suitability for endovascular graft fixation. *Eur J Vasc Endovasc Surg*. 1995;9:403–407.
9. Melas N, Saratzis A, Saratzis N, et al. Aortic and iliac fixation of seven endografts for abdominal-aortic aneurysm repair in an experimental model using human cadaveric aortas. *Eur J Vasc Endovasc Surg*. 2010;40:429–435.
10. Resch T, Malina M, Lindblad B, et al. The impact of stent design on proximal stent-graft fixation in the abdominal aorta: an experimental study. *Eur J Vasc Endovasc Surg*. 2000;20:190–195.
11. Avci M, Vos JA, Kolvenbach RR, et al. The use of endoanchors in repair EVAR cases to improve proximal endograft fixation. *J Cardiovasc Surg (Torino)*. 2012;53:419–426.
12. Jordan WD, de Vries JPPM, Ouriel K, et al. Midterm outcome of EndoAnchors for the prevention of endoleak and stent-graft migration in patients with challenging proximal aortic neck anatomy. *J Endovasc Ther*. 2015;22:163–170.
13. Perdikides T, Melas N, Lagios K, et al. Primary endoanchoring in the endovascular repair of abdominal aortic aneurysms with an unfavorable neck. *J Endovasc Ther*. 2012;19:707–715.
14. Jordan WD, Mehta M, Varnagy D, et al. Results of the ANCHOR prospective, multicenter registry of EndoAnchors for type Ia endoleaks and endograft migration in patients with challenging anatomy. *J Vasc Surg*. 2014;60:885–892.e2.
15. Donselaar EJ, van der Vijver-Coppen RJ, van den Ham LH, et al. EndoAnchors to resolve persistent type Ia endoleak secondary to proximal cuff with parallel graft placement. *J Endovasc Ther*. 2016;23:225–228.
16. Vries JPPM, Jordan WD. Improved fixation of abdominal and thoracic endografts with use of Endoanchors to overcome sealing issues. *Gefässchirurgie*. 2014;19:212–219.
17. Goudeketting SR, van Noort K, Vermeulen JJM, et al. Analysis of the position of EndoAnchor implants in therapeutic use during endovascular aneurysm repair. *J Vasc Surg*. 2019;69:1726–1735. doi:10.1016/j.jvs.2018.09.035
18. De Vries JPPM, Ouriel K, Mehta M, et al. Analysis of EndoAnchors for endovascular aneurysm repair by indications for use. *J Vasc Surg*. 2014;60:1460–1467.
19. Jordan WD, Mehta M, Ouriel K, et al. One-year results of the ANCHOR trial of EndoAnchors for the prevention and treatment of aortic neck complications after endovascular aneurysm repair. *Vascular*. 2016;24:177–186.
20. Goudeketting SR, Noort K Van, Ouriel K, et al. Influence of aortic neck characteristics on successful aortic wall penetration of EndoAnchors in therapeutic use during endovascular aneurysm repair. *J Vasc Surg*. 2018;68:1007–1016.
21. Tassiopoulos AK, Monastiriotes S, Jordan WD, et al. Predictors of early aortic neck dilatation after endovascular aneurysm repair with EndoAnchors. *J Vasc Surg*. 2017;66:45–52.
22. Patel R, Sweeting MJ, Powel JT, et al. Endovascular versus open repair of abdominal aortic aneurysm in 15-years' follow-up of the UK endovascular aneurysm repair trial 1 (EVAR trial 1): a randomized controlled trial. *Lancet*. 2016;388:2366–2374.
23. Muhs BE, Jordan W, Ouriel K, et al. Matched cohort comparison of endovascular abdominal aortic aneurysm repair with and without EndoAnchors. *J Vasc Surg*. 2018;67:1699–1707.
24. Arko FR, Heikkinen M, Lee ES, et al. Iliac fixation length and resistance to in-vivo stent-graft displacement. *J Vasc Surg*. 2005;41:664–671.
25. Veerapen R, Dorandeu A, Serre I, et al. Improvement in proximal aortic endograft fixation: an experimental study using different stent-grafts in human cadaveric aortas. *J Endovasc Ther*. 2003;10:1101–1109.